

# Colloid Particle Adsorption on Partially Covered (Random) Surfaces

Zbigniew Adamczyk,<sup>1</sup> Paweł Weroński, and Elizeusz Musiał

*Institute of Catalysis and Surface Chemistry, Polish Academy of Sciences, ul. Niezapominajek 8, 30-239 Cracow, Poland*

Received September 12, 2000; accepted April 2, 2001

**The random sequential adsorption (RSA) approach was used to model irreversible adsorption of colloid particles at surfaces precovered with smaller particles having the same sign of surface charge. Numerical simulations were performed to determine the initial flux of larger particles as a function of surface coverage of smaller particles  $\theta_s$  at various size ratios  $\lambda = a_1/a_s$ . These numerical results were described by an analytical formula derived from scaled particle theory. Simulations of the long-time adsorption kinetics of larger particles have also been performed. This allowed one to determine upon extrapolation the jamming coverage  $\theta_1^\infty$  as a function of the  $\lambda$  parameter at fixed smaller particle coverage  $\theta_s$ . It was found that the jamming coverage  $\theta_1^\infty$  was very sensitive to particle size ratios exceeding 4. Besides yielding  $\theta_1^\infty$ , the numerical simulations allowed one to determine the structure of large particle monolayers at the jamming state which deviated significantly from that observed for monodisperse systems. The theoretical predictions suggested that surface heterogeneity, e.g., the presence of smaller sized contaminants or smaller particles invisible under microscope, can be quantitatively characterized by studying larger colloid particle adsorption kinetics and structure of the monolayer.** © 2001 Academic Press

**Key Words:** adsorption of particles; colloid adsorption; heterogeneous surfaces; particle adsorption.

## INTRODUCTION

Adsorption and deposition (irreversible adsorption) of colloids and bioparticles at solid/liquid interfaces are of great significance in many natural and practical processes such as water and waste water filtration, membrane filtration, papermaking, flotation, protein and cell separation, enzyme immobilization, biofouling of membranes, and artificial organs. Often in these processes, especially in filtration, polydisperse suspensions or mixtures appear, e.g., colloid/polymer, colloid/macroscale particle, or protein/surfactant. As a result of their higher diffusivity the smaller components of the mixture will adsorb preferentially at the interface, forming a layer which may prohibit consecutive deposition of larger particles. This leads to a considerable decrease in the kinetics of larger particle accumulation at the interface as reported in the literature (1–3). Similar problems often appear in model experiments concerned with protein or colloid particle adsorption when the usual substrate cleaning

procedure may produce a nanosized contaminant layer difficult to detect by conventional means. Formation of such a layer will produce surface heterogeneity, in respect to both charge distribution and geometry, which is expected to influence the kinetics and maximum coverage of the proper adsorption experiments.

Despite the great significance of particle adsorption at heterogeneous surfaces, hereafter referred to for sake of brevity as random surfaces, few works have been devoted to this subject. A theoretical analysis was performed in (3, 4) for large-to-small particle size ratios 2.2, 5, and 10. These results have been confirmed in the kinetic aspects by the experiments performed with polystyrene latex particles adsorbing at surfaces precovered by smaller latex particles (3, 5). The larger-to-smaller particle size ratio was 2.2. In this paper we extend this theoretical analysis to a broader range of particle size ratios and determines the maximum coverage of larger particles adsorbing at random surfaces. The maximum or “jamming” coverage, of primary interest from the practical viewpoint, determines the maximum “capacity” of an interface.

## THE THEORETICAL MODEL

### General Considerations

Consider the situation shown in Fig. 1a, where a random surface is produced by covering a homogeneous interface by  $N_s$  small spherical particles of radius  $a_s$  adsorbed irreversibly at the distance  $\delta_m$  (primary minimum distance). The particle distribution is known *a priori* and can be quantitatively characterized in terms of the pair correlation function (called also radial distribution function)  $g(r)$ , where  $r$  is the radial distance between smaller particles. The simplest situation arises when  $g = 1$  for all distances, which corresponds to a perfectly random distribution of particles. This can easily be realized experimentally for low particle coverage defined as

$$\theta_s = \pi a_s^2 N_s / S, \quad [1]$$

where  $S$  is the geometrical area of the interface.

However, for  $\theta_s > 0.1$  deviations from the uniform distribution occur and particle positions become correlated, which manifests itself by increased number of pairs separated by small distances. The pair correlation function in this case is well known from numerical simulations (6) and from experiments (6–8).

<sup>1</sup> To whom correspondence should be addressed.

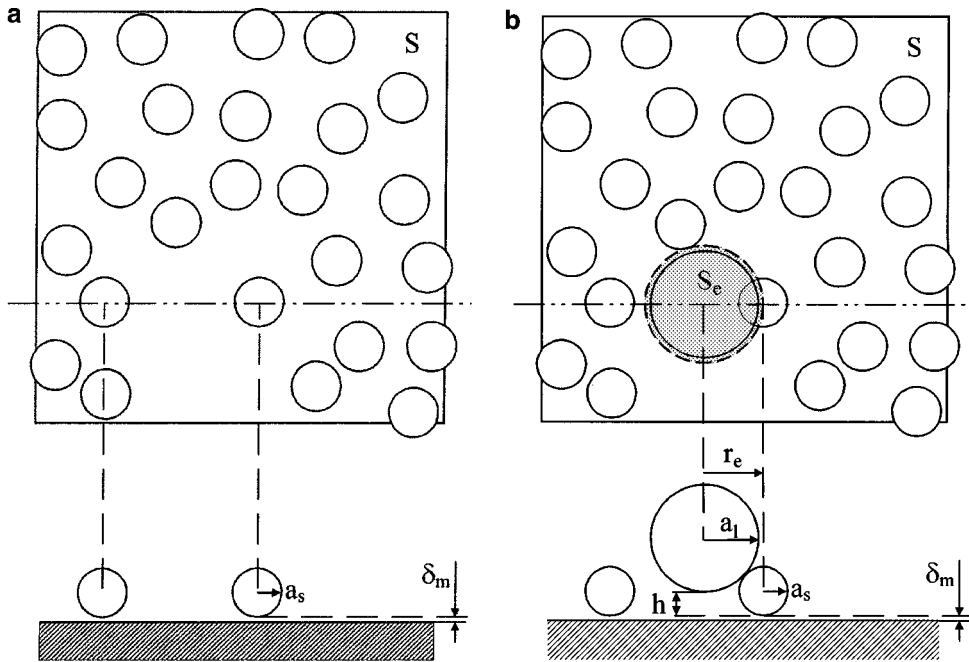


**FIG. 1.** (a) Random surface produced by irreversible adsorption of small particles of radius  $a_s$ . (b) Schematic view of larger particle adsorption on precovered surfaces with the definition of the exclusion area  $S_e$ .

Consider now adsorption of larger particles (having effective radius  $a_l$ ) over such a random surface. Assume that the large/small particle interactions are of the hard particle type; i.e., the net interaction energy  $\phi$  tends to infinity when the particles overlap and zero otherwise (9). This situation can be realized experimentally at high ionic strength if the small and large particles bear the same surface charge. According to this postulate, a large particle can be placed at distance  $h$  (see Fig. 1b) when there are no other particles within the circular area  $S_e$ , called the exclusion area. From simple geometry one can deduce that the size of the exclusion area is given by the expression

$$S_e = \pi r_e^2(h) = \pi[4a_s a_l + (2a_s - 2a_l - h)h], \quad [2]$$

where  $r_e$  is the radius of the exclusion area (see Fig. 1b). Obviously, for  $h = 0$  the exclusion area equals  $4\pi a_s a_l$ , whereas for  $h = 2a_s$ ,  $S_e = 0$ .

The probability of finding the empty area of size  $S_e$  averaged over the entire surface  $S$  (which equals the probability of placing a particle over the interface) is defined as the available surface function, ASF (10–13) called also the surface blocking function  $B$  (8–9). This function has fundamental significance for reversible (equilibrium) systems, allowing one to calculate the thermodynamic potential of particles (10). For irreversible systems considered in our work, the knowledge of the blocking function is necessary for a quantitative description of particle adsorption kinetics. Since the blocking function depends in a complicated manner on particle coverage, particle distribution, and the distance  $h$ , no theoretical results have been derived yet

for random surfaces. The only results in the form of a power expansion of  $B$  in terms of  $\theta$  were formulated for a monodisperse system and homogeneous surfaces (13). These results, discussed extensively in (9), indicate that the most significant contribution to the blocking effects come from the region close to the interface, when the adsorbing particles approach the primary minimum distance  $\delta_m$  ( $h \rightarrow 0$ ). In this limit, the blocking function can easily be calculated numerically for arbitrary  $\theta$  by applying the procedure described below.

Moreover, useful analytical expressions for the blocking function can be derived in this limit for some simple distributions of adsorbed particles. For example, assuming the binomial particle distribution, pertinent to the low coverage limit (14), one can calculate the averaged probability of finding an area of the size  $S_e$  without particles  $p_1$  (blocking function  $B_1^0$ ) from the equation

$$p_1 = B_1^0 = \left(1 - \frac{S_e}{S}\right)^{N_s} = \left(1 - \frac{S_e}{S}\right)^{\frac{S}{S_e} \langle n_s \rangle}, \quad [3]$$

where  $\langle n_s \rangle = N_s S_e / S = 4\lambda \theta_s$  is the average number of particles which should be expected statistically over the area  $S_e$ , and  $\lambda = a_l / a_s$  is the larger-to-smaller particle size ratio.

For most situations of practical interest the ratio  $S_e / S$  remains much smaller than unity, which means that the binomial distribution becomes the Poisson distribution and Eq. [3] transforms into the exponential form

$$B_1^0(\theta_s) = e^{-\langle n_s \rangle} = e^{-4\lambda \theta_s}. \quad [4]$$

As can be deduced from this equation, the adsorption probability of larger particles decreases exponentially with surface coverage of smaller particles, proportionally to the  $\lambda$  parameter. This means that at fixed  $\theta_s$ , the adsorption rate of larger particles becomes negligible for higher aspect ratio  $a_1/a_s$ .

It should be mentioned, however, that Eq. [4] remains valid for low  $\theta_s$  only when particle distribution remains uniform. A more accurate expression valid for broader range of  $\theta_s$  was derived in (4) by exploiting the scaled particle theory. It has the form

$$B_1^0(\theta_s) = (1 - \theta_s) \exp \left\{ -\frac{(4\lambda - 1)\theta_s}{1 - \theta_s} - \left[ \frac{(2\sqrt{\lambda} - 1)\theta_s}{1 - \theta_s} \right]^2 \right\}. \quad [5]$$

Equations [4] and [5] can be used as boundary conditions for the bulk transport equation describing large particle adsorption kinetics in a manner analogous to homogeneous systems (9, 15). In the limiting case of stationary transport under forced convection conditions (when the diffusion boundary thickness remains comparable with particle dimension) one can express the rate of large particle adsorption by the expression (9)

$$\frac{1}{\pi a_1^2} \frac{d\theta_1}{dt} \cong j_0 B_1^0(\theta_s), \quad [6]$$

where  $t$  is the time and  $j_0$  is the large particle flux in the absence of smaller particles. It was demonstrated experimentally in (3, 5) that Eq. [6] can be used as a reasonable approximation for describing colloid (polystyrene latex) particle adsorption at precovered surfaces.

However, Eqs. [4] and [5] describing the blocking function are valid only when there is no appreciable accumulation of larger particles at the interface so the surface exclusion effects stemming from larger particles remain negligible. A proper evaluation of the blocking parameter, particle adsorption kinetics, and their distribution in this case can be achieved only by numerical simulations described below.

### The Simulation Algorithm

The irreversible adsorption of larger particles was simulated theoretically in terms of the random sequential adsorption (RSA) model developed in (12–14, 16, 17). According to this approach, particles of various sizes or geometrical shapes are placed randomly, one at a time, over a plane (interface) of isotropic properties. Once an empty surface element of the size  $S_c$  is found, the particle becomes permanently attached with no consecutive motion allowed. Otherwise it is rejected and a new addition attempt is undertaken, uncorrelated with previous attempts. The process is continued until the jamming state is reached when no additional particles can be placed over the simulation plane. It is interesting to mention that for hard spherical particles adsorbing over homogeneous surfaces the jamming coverage equals 0.547 (16–17).

The classical RSA model formulated for hard particles can be extended to particles interacting via the exponentially decaying potential stemming from the double-layer repulsion (6, 18). Similarly, one can extend this model by considering particle transport through the adsorbed particle layer (13), which affects kinetic aspects of particle adsorption. However, as demonstrated in (19) the jamming state remains practically unaffected if particle diffusion effects are introduced into the RSA model.

In this work, therefore, we used the calculation algorithm based on the classical RSA model (3–6, 12, 18). The simulations were carried out over a square adsorption plane with the usual periodic boundary conditions at its perimeter. As in previous works (3–6, 20) the simulation plane was divided into subsidiary square areas (cells) of the size  $\sqrt{2}a_s$ , which ensures that only one particle can be placed within the cell. The subdivision procedure enhanced the efficiency of the overlapping test performed at each simulation step. The entire simulation procedure consisted of two main stages:

(i) First the homogeneous simulation plane was covered with smaller sized particles to a prescribed surface coverage  $\theta_s$ . During this stage the usual RSA simulation algorithm pertinent to hard spheres was used.

(ii) The random (heterogeneous) surface produced in the first stage was then covered with larger spheres (adsorbing at the primary minimum distance  $\delta_m$ ) by choosing at random their position over the simulation area. The overlapping test between larger/larger and larger/smaller particles was carried out by checking if the conditions

$$r_{11}/a_1 > 2 \quad \text{and} \quad r_{1s}/a_1 > 1 + \frac{1}{\lambda}$$

were met simultaneously (where  $r_{11}$  is the distance between larger particle centers and  $r_{1s}$  is the distance between large/small particle centers).

The above algorithm enabled one to simulate kinetics of larger particle adsorption by defining the dimensionless quasi-time variable

$$\tau = N_{\text{att}}/N_{\text{ch}} = \pi a_1^2 N_{\text{att}}, \quad [7]$$

where  $N_{\text{att}}$  is the overall number of attempts to place larger particles over the simulation plane and  $N_{\text{ch}} = 1/\pi a_1^2$  is the characteristic number of particles. Due to computer limitations the maximum dimensionless time in our simulations reached  $10^4$ , which required about  $10^9$  simulation steps. Therefore, in order to calculate the jamming coverage (after infinite adsorption time) the results obtained for long time  $\tau$  have been extrapolated by using a power law dependence.

The adsorption probability of larger particles (blocking parameter  $B_1^0$ ) was calculated according to the definition

$$B_1^0(\theta_s) = N_{\text{succ}}/N_{\text{att}}, \quad [8]$$

where  $N_{\text{succ}}$  is the number of successful adsorption events performed at fixed  $\theta_s$  and  $N_{\text{att}}$  is the overall number of attempts at placing larger particles at the surface precovered with smaller particles. In practice, the value of  $B_1^0(\theta_s)$  converged when the number of adsorption attempts exceeded  $10^5$ .

For calculating the pair correlation function a population having  $N_1$  larger particles adsorbed over the interface of the area  $S$  was generated by using the above RSA scheme. Then, the  $g_1$  function was determined for a discrete set of distances from the formula

$$g_1(r) = \frac{\pi a_1^2}{\theta_1} \left( \frac{\Delta N_1}{2\pi r \Delta r} \right), \quad [9]$$

where  $\Delta r$  is the thickness of the annulus,  $\Delta N_1$  is the averaged number of particles adsorbed within the annulus  $2\pi r \Delta r$  drawn around a central particle, and  $\theta_1 = \pi a_1^2 N_1 / S$  is the averaged coverage of larger particles. In order to increase the accuracy of pair correlation function calculations, additional averages from many populations have been taken so the overall number of larger particles reached 70,000.

## RESULTS AND DISCUSSION

Due to the simplicity of the RSA algorithm, numerical simulations for large particle populations can be performed, enabling one to determine with good accuracy both the kinetics of particle adsorption and the structure of transient monolayers up to the jamming limit.

The quantity of considerable interest is the blocking function  $B_1^0$  that characterizes initial adsorption kinetics of larger particles at precovered surfaces. In Fig. 2 the dependence of this function on surface coverage of smaller particles is shown for  $\lambda = 2.2, 5,$  and  $10$ . As can be noticed the influence of preadsorbed smaller particles on the initial flux ( $B_1^0$  function) is significantly more pronounced for larger values of the  $\lambda$  parameter. It is interesting to note that the numerical data are well reflected for practically the entire range of  $\theta_s$  by the analytical Eq. [5]. On the other hand, Eq. [4] remains an accurate approximation for  $\theta_s < 0.1$ , i.e., in the case when the smaller particle distribution remains uniform. The theoretical predictions shown in Fig. 2 suggest that the presence of trace amounts of small particles often invisible under an optical microscope can exert a profound effect on adsorption kinetics (initial flux) of larger particles, whose surface concentration can easily be measured directly (microscopically). One may therefore expect that by measuring the initial flux  $j_0$  of larger particles (of various sizes) one can detect the presence of smaller (invisible) particles. However, a quantitative determination of the surface coverage of these particles becomes possible only by considering the coupling between the surface layer transport (described by the function  $B_1^0$ ) and the bulk transport (governed by convective diffusion of particles). As shown in (9) particle flux  $j$  in this case is governed by the

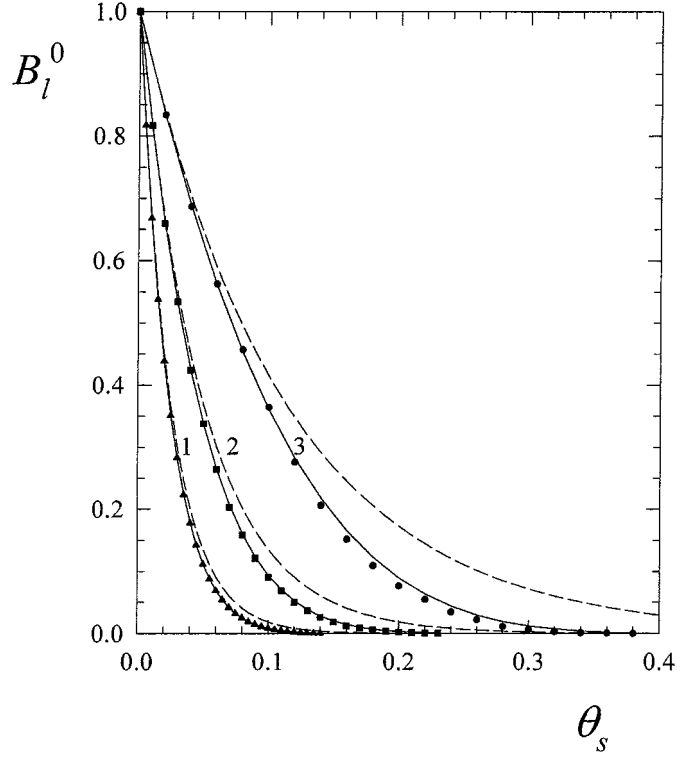


**FIG. 2.** Dependence of  $B_1^0$  on surface coverage of smaller particles  $\theta_s$ . The points denote numerical simulations performed for (1)  $\lambda = 10$ , (2)  $\lambda = 5$ , (3)  $\lambda = 2.2$ . The continuous lines denote the analytical results calculated from Eq. [5] and the broken lines represent the results calculated from Eq. [4].

generalized blocking function

$$\overline{B_1^0}(\theta_s) = j/j_0 = \frac{K B_1^0(\theta_s)}{1 + (K - 1) B_1^0(\theta_s)}, \quad [10]$$

where  $K = k_a/k_b$ ,  $k_a$  is the kinetic adsorption constant given by the equation

$$k_a = \frac{1}{\int_{\delta_m}^{\delta} \frac{e^{\phi_1/kT}}{D(h')} dh'}, \quad [11]$$

where  $\delta$  is the thickness of the adsorbed smaller particle layer,  $\phi_1$  is the interaction energy of the larger particle with the interface,  $k$  is the Boltzmann constant,  $T$  is the absolute temperature,  $D$  is the position dependent diffusion coefficient of the particle (20), and  $h' = h + \delta_m$  and  $k_b$  is the bulk mass transfer rate which can be calculated analytically or numerically for stationary transport to the uniformly accessible surfaces such as a rotating disk, impinging jet cells, etc. (8, 21).

Assuming the perfect sink interaction model and expressing the diffusion coefficient as  $D = D_\infty h' / (h' + a_1)$  (19), where  $D_\infty$  is the diffusion coefficient of the particle in the bulk, one can

evaluate  $k_a$  explicitly to obtain

$$K = \frac{1}{\text{Sh} \left( \ln \frac{\delta}{\delta_m} + \frac{2}{\lambda} \right)}, \quad [12]$$

where  $\text{Sh} = k_b \frac{a_1}{D_\infty}$  is the dimensionless mass transfer Sherwood number.

As can be deduced from Eq. [10], the larger particle flux (normalized to the flux for a uncovered surface) depends on two unknown parameters only, i.e.,

$$j/j_0 = f(\theta_s, a_s). \quad [13]$$

This suggest that by measuring  $j/j_0$  experimentally for a series of large particle sizes, one can determine both the coverage  $\theta_s$  and the radius  $a_s$  of smaller particles using a nonlinear fitting procedure.

However, from Eq. [5] one can deduce that this is feasible for not too large  $\theta_s$  and  $a_1/a_s$  values. Otherwise, the larger particle flux becomes dependent only on the product  $\lambda\theta_s$ , which excludes simultaneous determination of these parameters. In this case one can determine either the smaller particle size (if the coverage is known) or the coverage  $\theta_s$  if particle size is known or can be estimated. In the latter case, using Eq. [4] one can derive the following analytical expression for calculating  $\theta_s$  using the measured  $j/j_0$  value,

$$\theta_s = \frac{1}{4\lambda} \ln \frac{K - (K - 1)j/j_0}{j/j_0}. \quad [14]$$

Some experimental data obtained for latex particles (9) confirmed the validity of the above model, in particular Eq. [10], for predicting adsorption flux of larger particles at precovered surfaces in the case of  $\lambda = 2.2$ .

The data shown in Fig. 2 and Eqs. [10]–[13] are valid for the initial adsorption stage when the flux of larger particles remains steady. For longer times, however, the accumulation of larger particles will lead to surface blocking effects, which decrease their adsorption rate and influence adsorption kinetics. The typical kinetic curves ( $\theta_1$  vs  $\tau$  dependencies) obtained in this case for  $\lambda = 5$ ,  $K = 1$  and various concentrations of smaller particles  $\theta_s$  are plotted in Fig. 3. As can be seen, for low  $\tau$  the adsorption curves are indeed linear with the slope (initial flux) well reflected by Eq. [5]. However, for longer times, when  $\theta_s > 0.1$  the kinetic curves deviate significantly from linearity, indicating that the adsorption rate decreases. In order to present this long-time adsorption data more efficiently we applied the  $\theta_s$  vs  $\tau^{-1/2}$  transformation which compresses the infinite time domain into a finite one. This transformation has been used previously (6, 12, 16–17) for analyzing adsorption at homogeneous surfaces. As can be seen in Fig. 3, the numerical results plotted using this transformation can indeed be described by a straight-line dependence, although the range of this asymptotic regime is decreasing for higher values of  $\theta_s$ . The linear dependence of  $\theta_s$  on  $\tau^{-1/2}$  implies that the blocking parameter of larger particles

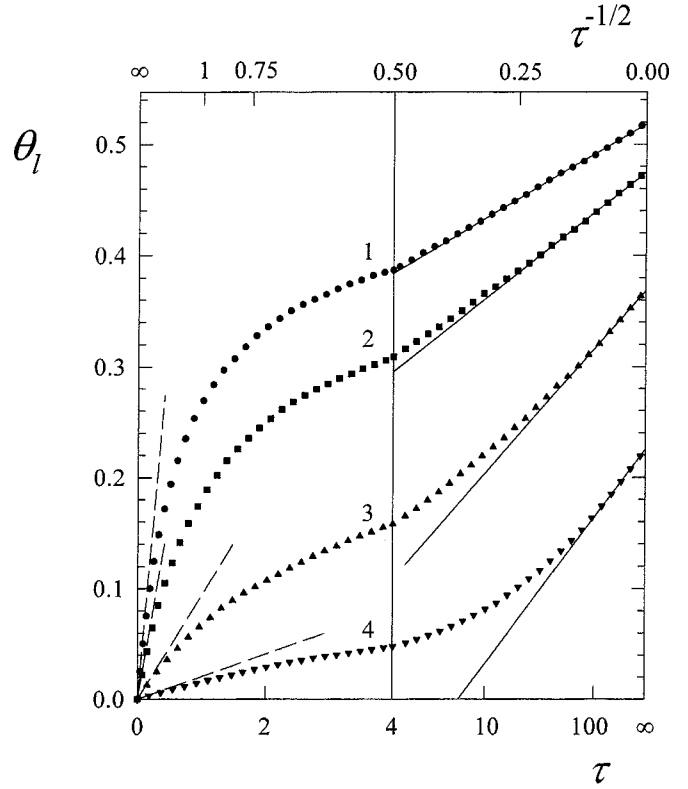


**FIG. 3.** Kinetics of larger particle adsorption at surfaces precovered with smaller particles expressed as  $\theta_1$  vs  $\tau$  dependencies;  $\lambda = 5$ . (1)  $\theta_s = 0$ , (2)  $\theta_s = 0.02$ , (3)  $\theta_s = 0.05$ , (4)  $\theta_s = 0.10$ . The broken lines denote the analytical results calculated as  $\theta_1 = B_1^0 \tau$  with  $B_1^0$  given by Eq. [5] and the solid lines denote the linear fits, i.e.,  $\theta_1^\infty - \theta_1 \sim \tau^{-1/2}$ .

$B$  is given by the expression (4)

$$B_1 \sim [\theta_1^\infty - \theta_1]^3, \quad [15]$$

where the jamming coverage of larger particles  $\theta_1^\infty$  is dependent only on the initial coverage of smaller particles  $\theta_s$ . Thus, the jamming coverage has been calculated by fitting the numerical data (the  $\theta_1$  vs  $\tau^{-1/2}$  dependencies) by straight lines and subsequent extrapolation to  $\tau^{-1/2} \rightarrow 0$  (adsorption time tending to infinity). Averages from five various computer runs have been taken in order to attain a sufficient precision of  $\theta_1^\infty$ . Calculations have been performed for  $\lambda$  changed within 1 to 20 at fixed values of  $\theta_s$  equal to 0.02, 0.05, 0.10, and 0.2. The results of these calculations are collected in Fig. 4. One can observe in this figure that the presence of preadsorbed particles decreases monotonically the jamming coverage of larger particles, although the effect becomes well pronounced only for  $\lambda > 4$  and  $\theta_s > 0.02$ . For example, for  $\theta_s = 0.05$  the change in the  $\lambda$  parameter from 5 to 20 results in decrease of  $\theta_1$  from 0.47 to 0.35. The net coverage  $\theta_1 + \theta_s$  drops in this case from 0.52 to 0.40. On the other hand, for  $\theta_s = 0.1$  the change in the  $\lambda$  parameter from 5 to 20 will exert a more significant effect on  $\theta_1$  which will decrease from 0.37 to 0.02, whereas the net coverage decreases from 0.47 to 0.12.

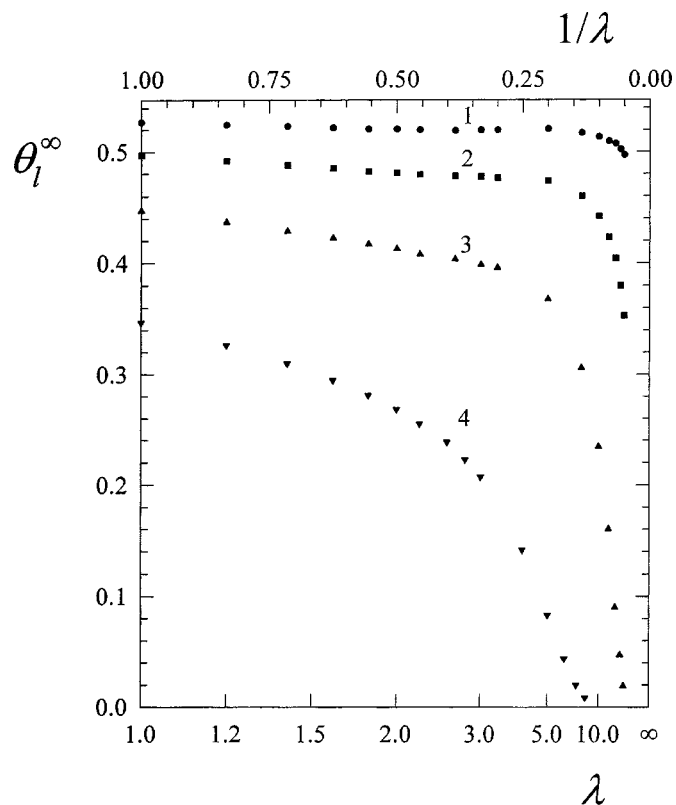


**FIG. 4.** Dependence of the jamming concentration of larger particles  $\theta_l^\infty$  on  $\lambda = a_l/a_s$  and  $1/\lambda$  parameters determined numerically for fixed concentration of smaller particles. (1)  $\theta_s = 0.02$ , (2)  $\theta_s = 0.05$ , (3)  $\theta_s = 0.1$ , (4)  $\theta_s = 0.2$ .

The abrupt change in  $\theta_l$  upon increase in  $\lambda$  or coverage of smaller particles  $\theta_s$ , (analogous to the change in the initial flux presented in Fig. 2) suggests that by measuring  $\theta_l$  experimentally one can draw conclusions about the size and coverage of smaller sized particles. This means that surface homogeneity can easily be determined in measurements of such type. One should mention, however, that the jamming coverage measurements are considerably more tedious than the kinetic measurements of the initial flux of larger particles.

The presence of preadsorbed particles affects not only the kinetic aspects of larger particle adsorption but also the distribution of larger particle monolayers. This can be qualitatively observed in Fig. 5, where the “mixed” monolayers are shown obtained from numerical simulations for a fixed larger particle coverage equal to 0.1 and various  $\lambda$  equal to 2.2, 5, and 10. It should be noted that for  $\lambda > 4$ , adsorption of larger particles may occur in such a way that the smaller particles are located underneath (shown in Fig. 5 by empty circles). This phenomenon reduces the surface blocking effect in comparison with adsorption of disks analyzed previously (22–23).

In Fig. 6 larger particle monolayers are presented for  $\lambda = 1$  (reference system of monodisperse spheres), 2.2, 5, and 10. The smaller particles are not shown, which can mimic the experimental situation when only the larger particles are visible (e.g., under optical microscope). One can qualitatively notice in Fig. 6

that the monolayer structure is dependent on the  $\lambda$  parameter. Quantitatively, this can be demonstrated by determining the pair correlation function of larger particles  $g_l$  according to the method described above. The results are shown in Fig. 7. As can be seen, for all  $\lambda$  the shape of the pair correlation function deviates considerably from the monodisperse counterpart ( $\lambda = 1$ ), being close to unity for all distances. This is especially well

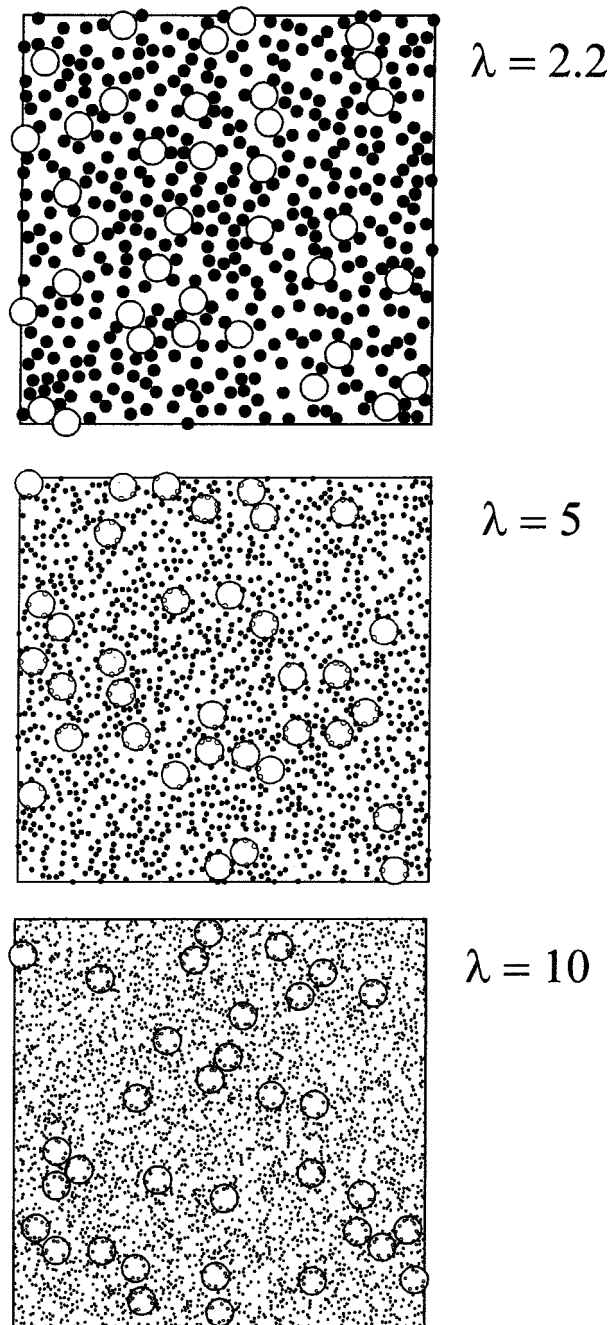


**FIG. 5.** The adsorbed particle “monolayers” close to the jamming limit simulated numerically for  $\theta_l = 0.1$  and various  $\lambda$ , i.e.,  $\lambda = 2.2$ ,  $\theta_s = 0.3$ ;  $\lambda = 5$ ,  $\theta_s = 0.2$ ;  $\lambda = 10$ ,  $\theta_s = 0.14$ . The smaller particle fragments located below larger particles are marked by empty circles.

pronounced for  $\lambda = 2.2$  when the  $g_1$  function exhibits a maximum of height 1.5 located at the dimensionless distance  $r_1/a_1$  about 2.7. The position of this maximum agrees quite well with the separation distance between two larger particles with one smaller particle in between, which from simple geometry can be calculated as  $4/\sqrt{\lambda}$ . Thus, for  $\lambda = 2.2$ ,  $r_1/a_1$  equals 2.65, which agrees quite well with the above value determined from simulations. From simple geometrical considerations one can also deduce that for  $\lambda = 5$  the smaller particles cannot prevent the larger ones from approaching each other closely. Thus, the secondary maximum of the  $g_1$  function should be absent which is confirmed by the data presented in Fig. 7.

The results concerning the distribution of larger particles over a random monolayer shown in Figs. 5–7 suggest, therefore, that the presence of smaller particles (causing surface heterogeneity) may be detected by determining the pair correlation functions of larger particles, used as markers. One should remember, however, that the differences in monolayer structure are most pronounced for larger particle coverage close to jamming, which makes such measurements rather tedious.

It should also be mentioned that all theoretical data presented in this work are strictly valid for hard particles, i.e., for the case when the repulsive interaction range remains much smaller than particle size  $a_s$ . This situation can be realized experimentally for high ionic strength of particle suspension, which is usually

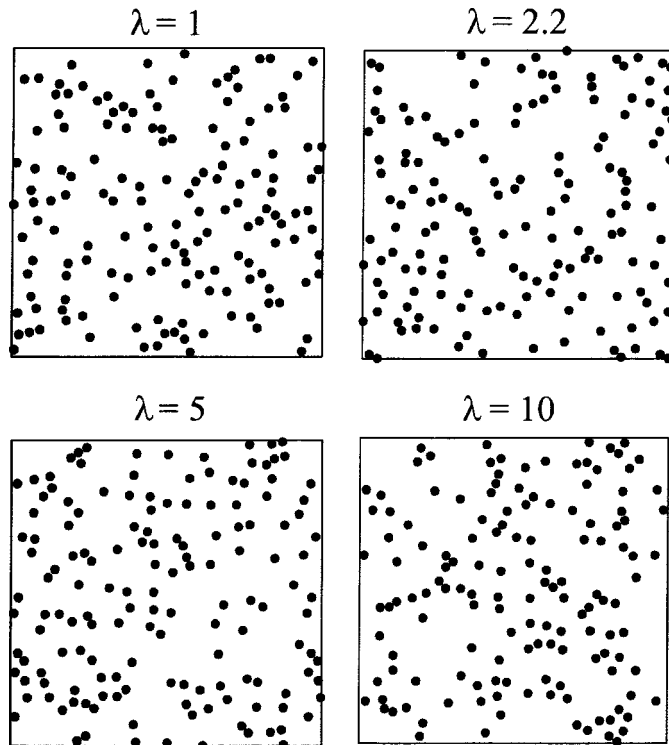


**FIG. 6.** The larger particle “monolayers” close to the jamming limit simulated numerically for  $\theta_1 = 0.1$  and various  $\lambda$  (the smaller particles are not shown):  $\lambda = 1$  (reference monodisperse system);  $\lambda = 2.2$ ,  $\theta_s = 0.3$ ;  $\lambda = 5$ ,  $\theta_s = 0.2$ ;  $\lambda = 10$ ,  $\theta_s = 0.14$ .

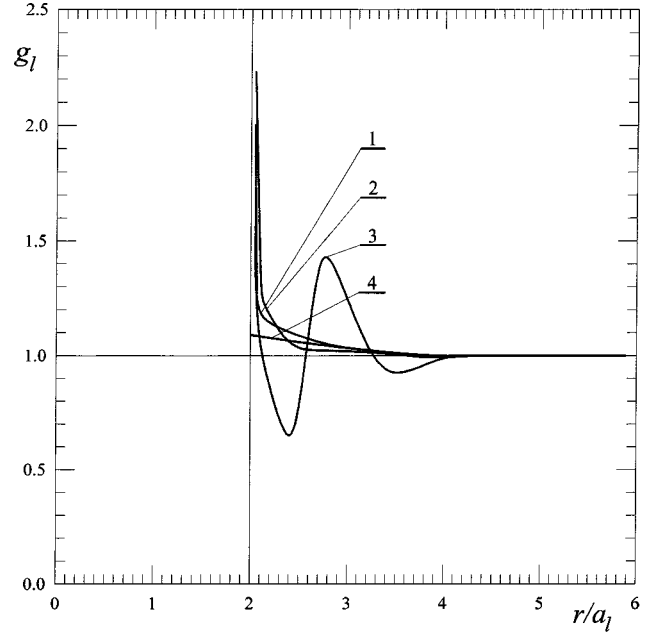


**FIG. 7.** The pair correlation function of larger particles  $g_l$  derived from numerical simulations for  $\theta_1 = 0.1$  and various  $\lambda$ , i.e., (1)  $\lambda = 10$ , (2)  $\lambda = 5$ , (3)  $\lambda = 2.2$ , (4)  $\lambda = 1$ .

the case in protein adsorption studies mimicking physiological conditions. However, for lower ionic strength the interaction range may become comparable with particle dimensions. In this case the above data pertinent to hard particle systems can still be used for estimating adsorption phenomena by introducing the effective hard particle concept discussed extensively elsewhere (6, 8–9). According to this approach the geometrical size of an interacting particle is increased by the effective interaction range  $h^*$  strictly related to the double-layer thickness. In practice, for particle size range 0.01–0.1  $\mu\text{m}$ , one can assume that  $h^*$  is proportional to the double-layer thickness with the coefficient  $\xi$  varying between 1.5 and 2.5. Knowing  $h^*$  for smaller and larger particles one can exploit the above results derived for hard spheres for calculating the effective coverage from the equation

$$\theta_s^* = \theta_s(1 + h_1^*/a_1)(1 + h_s^*/a_s). \quad [16]$$

In this way, Eqs. [4] and [5] can be used for predicting the initial adsorption rate of larger particles interacting via a repulsive double-layer potential over random surfaces. However, the transformation of the jamming coverage to interacting particle systems seems more complicated without additional simulations performed for interacting particles.

## CONCLUDING REMARKS

It was demonstrated theoretically that adsorption of colloid particles at random surfaces is considerably reduced in comparison with uniform surfaces. This effect is primarily governed by

the  $\lambda = a_l/a_s$  parameter (particle size ratio) and the degree of coverage of smaller particles  $\theta_s$ . The initial flux of larger particles can be well approximated for the entire range of  $\lambda$  and  $\theta_s$  by the analytical Eq. [5]. On the other hand, for  $\theta < 0.1$  Eq. [4] can be used with good accuracy, indicating that the initial flux decreases exponentially with the  $\lambda\theta_s$  product.

As demonstrated numerically, for longer times, adsorption kinetics at random surfaces is governed by the power-law dependence, i.e.,

$$\theta_1^\infty - \theta_1 \sim \tau^{-1/2},$$

where the jamming coverage of larger particle  $\theta_1^\infty$  (depending on  $\theta_s$  and  $\lambda$ ) was found by extrapolation. The  $\theta_1^\infty$  values for random surfaces are considerably smaller, especially for  $\lambda > 5$ , than the limiting value of 0.547 pertinent to uniform surface adsorption.

It was also predicted theoretically that the structure of particle monolayers at random surfaces (characterized in terms of the pair correlation function  $g_1$ ) differs significantly from that observed at homogeneous surfaces at the same coverage  $\theta_1$ .

The theoretical calculations enabled one to draw the conclusion that surface heterogeneity, e.g., the presence of smaller sized contaminants or smaller particle invisible under microscope can be quantitatively characterized by studying larger colloid particle adsorption kinetics (initial flux), the jamming coverage, and the pair correlation function.

#### ACKNOWLEDGMENT

This work was partially supported by KBN Grant 3T09A 105 18.

#### REFERENCES

1. Boluk, M. Y., and van de Ven, T. G. M., *Colloids Surf.* **46**, 157 (1990).
2. van de Ven, T. G. M., and Kelemen, S. J., *J. Colloid Interface Sci.* **181**, 118 (1996).
3. Adamczyk, Z., Siwek, B., Weroński, P., and Zembala, M., *Progr. Colloid Polymer Sci.* **111**, 41 (1998).
4. Adamczyk, Z., and Weroński, P., *J. Chem. Phys.* **108**, 9851 (1998).
5. Adamczyk, Z., Siwek, B., and Weroński, P., *J. Colloid Interface Sci.* **195**, 261 (1997).
6. Adamczyk, Z., Zembala, M., Siwek, B., and Warszyński, P., *J. Colloid Interface Sci.* **140**, 123 (1990).
7. Johnson, C. A., and Lenhoff, A. M., *J. Colloid Interface Sci.* **179**, 587 (1996).
8. Adamczyk, Z., Siwek, B., Zembala, M., and Belouschek, P., *Adv. Colloid Interface Sci.* **48**, 151 (1994).
9. Adamczyk, Z., and Weroński, P., *Adv. Colloid Interface Sci.* **83**, 137 (1999).
10. Reiss, H., Frish, H. L., and Lebowitz, J. L., *J. Chem. Phys.* **31**, 369 (1959).
11. Widom, B., *J. Chem. Phys.* **44**, 3888 (1966).
12. Schaaf, P., and Talbot, J., *J. Chem. Phys.* **91**, 4401 (1989).
13. Adamczyk, Z., Senger, B., Voegel, J. C., and Schaaf, P., *J. Chem. Phys.* **110**, 3118 (1999).
14. Adamczyk, Z., and Weroński, P., *J. Chem. Phys.* **107**, 3697 (1997).
15. Adamczyk, Z., and Szyk, L., *Langmuir* **16**, 5730 (2000).
16. Hinrichsen, E. L., Feder, J., and Jossang, T., *J. Stat. Phys.* **44**, 793 (1986).
17. Evans, J. W., *Rev. Mod. Phys.* **65**, 1281 (1993).
18. Adamczyk, Z., and Weroński, P., *J. Colloid Interface Sci.* **189**, 348 (1997).
19. Senger, B., Schaaf, P., Voegel, J. C., Johnner, A., Schmitt, A., and Talbot, J., *J. Chem. Phys.* **97**, 3813 (1992).
20. Adamczyk, Z., Siwek, B., Zembala, M., and Weroński, P., *J. Colloid Interface Sci.* **185**, 236 (1997).
21. Adamczyk, Z., Warszyński, P., Szyk-Warszyńska, L., and Weroński, P., *Colloids Surf. A* **165**, 157 (2000).
22. Talbot, J., and Schaaf, P., *Phys. Rev. A* **40**, 422 (1989).
23. Meakin, P., and Jullien, R., *Phys. Rev. A* **46**, 2029 (1992).